

Conduit dynamics and post-explosion degassing on Stromboli: a combined UV camera and numerical modelling treatment

Pering, T. D.^{*a}, McGonigle, A. J. S.^{a,d}, James, M. R.^b, Tamburello, G.^c, Aiuppa, A.^{c,d}, Delle Donne, D.^c, Ripepe, M.^c

*Corresponding author: T. D. Pering, Department of Geography, University of Sheffield, Sheffield, South Yorkshire, S10 2TN, UK. (ggp12tdp@sheffield.ac.uk)

^aUniversity of Sheffield, Dept. of Geography, Winter Street, S10 2TN, United Kingdom

^bLancaster Environment Centre, Lancaster University, Lancaster, LA1 4YQ, UK

^cDiSTeM, Università di Palermo, via Archirafi, 22, 90123 Palermo, Italy

^dIstituto Nazionale di Geofisica e Vulcanologia, Sezione di Palermo, Via Ugo La Malfa, 153, 90146, Palermo, Italy

^eDipartimento di Scienze della Terra, Università di Firenze, Via La Pira, 4, 50121, Firenze, Italy

Abstract

Recent gas flux measurements have shown that strombolian explosions are often followed by periods of elevated flux, or ‘gas codas’, with durations of order a minute. Here, we present UV camera data from 200 events recorded at Stromboli volcano to constrain the nature of these codas for the first time, providing estimates for combined explosion plus coda SO₂ masses of $\approx 18 - 225$ kg. Numerical simulations of gas slug ascent show that substantial proportions of the initial gas mass can be distributed into a train of ‘daughter bubbles’ released from the base of the slug, which we suggest, generate the codas, on bursting at the surface. This process could also cause transitioning of slugs into cap bubbles, significantly reducing explosivity. This study is the first attempt to combine high temporal resolution gas flux data with numerical simulations of conduit gas flow to investigate volcanic degassing dynamics.

Strombolian eruptions, gas slugs, uv cameras, gas flux, daughter bubbles, computational fluid dynamics

Key Points:

- Stromboli gas flux data suggest that trains of daughter bubbles may follow gas slugs
- CFD models suggest a complex relationship between daughter bubble production rate and N_f
- Bubble production can result in significant mass loss from ascending slugs

1. Introduction

Strombolian explosions are the archetypal events which occur every few minutes [Ripepe et al., 2002] at Stromboli volcano (Aeolian Islands, Italy) and are thought to result from the ascent and bursting of gas slugs [e.g., Chouet 1974; Blackburn et al. 1976; Seyfried and Freundt, 2000 and references therein]. Thus, the study of slug flow dynamics is pivotal to understanding the processes driving strombolian eruptions, and analytical and computational fluid dynamic (CFD) models have been

This article has been accepted for publication and undergone full peer review but has not been through the copyediting, typesetting, pagination and proofreading process which may lead to differences between this version and the Version of Record. Please cite this article as doi: 10.1002/2016GL069001

developed to help interpret geophysical signals [e.g., James et al. 2004, 2008; O'Brien and Bean, 2008; Del Bello et al. 2012].

With the advent of ultra-violet (UV) cameras [e.g., Mori and Burton, 2006; Bluth et al., 2007; Tamburello et al., 2011], gas fluxes can now be measured at sufficiently high temporal resolutions to also provide insight into slug fluid dynamics. Such data have recently enabled the identification of gas flux coda for the first time, which are periods of elevated emissions following individual strombolian events [Tamburello et al. 2012]. Coda are potentially produced from trains of 'daughter bubbles' that have been released from, and subsequently follow, the base of ascending slugs. Here, we use CFD models of slug ascent and daughter bubble production as a first step to quantify this process and assess its wider implications for conduit fluid dynamics.

The morphology and behaviour of ascending gas slugs depend on parameters which include conduit radius, magma density, and magma viscosity. Notably, magma viscosity and conduit radius also play key roles in determining the form and the degree of turbulence in the wakes that follow slugs [e.g. Campos and Guedes de Carvalho, 1988]. For long slugs, wake form has been shown to be a function of the dimensionless inverse viscosity, N_f , which represents a ratio of external forces to internal viscous forces:

$$N_f = \frac{\rho_m}{\mu} \sqrt{g(2r_c)^3}, \quad (1),$$

where ρ_m is the liquid density, μ is liquid viscosity, g is acceleration due to gravity, and r_c is tube radius [Campos and Guedes de Carvalho, 1988; Noguiera et al., 2006]. For N_f values < 500 slug wakes are closed (recirculatory) and axisymmetric, while for values > 500 , symmetry is lost and wakes become increasingly open and turbulent [Noguiera et al., 2006]. With sufficient wake turbulence, gas can be removed from the main slug by bubbles being sheared from its base [Wallis, 1969; Campos and Guedes de Carvalho, 1988]. The resulting 'daughter bubbles' can then either become entrained within the slug wake and subsequently re-incorporated back into the slug [Campos and Guedes de Carvalho, 1988], or can be ejected from the wake, to rise independently from, and behind, the main slug [e.g., Bouche et al. 2010]. To the authors' knowledge, Fernandes et al. (1983) detail the only previous attempt to quantify gas mass loss from the base of slugs, but did not consider the subsequent escape of the gas from the wake.

In the volcanic literature, daughter bubble production has been discussed briefly [e.g., James et al. 2006; Suckale et al. 2010; Llewellyn et al. 2014], but the implications for strombolian eruptions have yet to be quantified. Using values of 2700 kg m^{-3} for magma density [e.g., Vergnolle and Brandeis, 1996; Métrich et al., 2001], $200 - 500 \text{ Pa s}^{-1}$ for magma viscosity [Vergnolle et al. 1996] and $1 - 3 \text{ m}$ for conduit radius [e.g. Harris and Stevenson, 1997; Delle Donne and Ripepe, 2012], to represent the system at Stromboli, Equation 1 gives N_f values of $47 - 621$, suggesting that daughter bubble production could be possible. Therefore, motivated by the observed gas coda signals in UV camera measurements of eruptions at Stromboli, we report here on the use of CFD models to explore the potential effects of daughter bubble generation on strombolian eruptions. This is the first reported attempt to combine high temporal resolution volcanic gas flux data with numerical simulations of gas flow in conduits to investigate the dynamics of volcanic degassing.

2. UV Camera Measurements of SO₂ flux

We first characterised and quantified the gas release from a total of 200 events, which were categorised into two classes: Vent 1 events, numbering 120, which arose from the craters (mostly the south east crater; SEC), and Vent 2 events, numbering 80 and emanating from a hornito on the edge of the SEC. Vent 1 events were relatively ash-free, included the ejection of bombs and were associated with very long period (VLP) seismic signals while Vent 2 events released gas only and did not always produce a VLP signal (see Fig. 1e for VLP during a Vent 2 event). Events of both types occurred every $\approx 2 - 10$ minutes, with impulsive gas release lasting $\approx 10 - 30$ s in each case. The gas flux measurements were performed on the 11th, 13th, 21st, 22nd, 23rd, 25th June, and the 3rd July, 2014, using the permanent UV camera network installed by the Università di Palermo and Università di Firenze, within the framework of the FP7-ERC project “BRIDGE”. The cameras imaged the entire crater terrace, and gas fluxes were determined ≈ 50 m above the vents.

Fig. 1 shows example integrated column amounts of SO₂ and gas velocities (calculated using optical flow algorithms [e.g., Horn and Schunk, 1981; Peters et al. 2015]), which were used to calculate SO₂ fluxes. The data used to characterise each event were taken from the base of initial flux peak until measured flux values returned to background levels. SO₂ masses for the explosions were calculated by integrating underneath the peaks of each flux trace associated with the initial impulsive gas release (see movie S1 and text in S2 for further details) and, for coda masses, until flux levels returned to background levels; see S2 for examples (also see Fig. 1, Kantzas et al. [2010]; Tamburello et al. [2011, 2012] and references therein, for full details on UV camera calibration, and image processing).

To facilitate comparison of all measured Vent 1 and 2 events, the explosive traces were normalised by subtracting each event's minimum value, then dividing by the maximum. The normalised data show a range of characteristics, and events can be visually separated into a number of distinct families (Fig. 2). Each event shows an initial peak in flux, followed by a flux coda [e.g., Tamburello et al. 2012]. Additional observed features include a variable number of subsequent flux peaks within the coda, of differing magnitudes and coda durations.

In general, SO₂ masses were an order of magnitude larger for Vent 1 events than for the Vent 2 events, in both the main explosion (Fig. 1h) and coda (Fig. 1f, and g) components (see Table S1 in supplementary information for further detail and for total gas masses calculated using the gas chemical compositions from Burton et al. [2007]). The latter compositional data pertain to Vent 1 type activity alone, therefore the Vent 2 total masses must be considered best estimates on the basis of available data. For the Vent 2 events, with increasing explosion mass, a higher proportion of the overall released mass is contained within the explosion (Fig. 1h). For Vent 1 events, a similar relationship exists, but this appears somewhat skewed by events with rather low coda masses (Fig. 1h).

3. CFD modelling of slug flow and gas flux

To explore the potential for daughter bubble production as a source for gas coda, slug ascent was simulated using the computational fluid dynamics package Ansys Fluent[®]. A series of 3D models were constructed based on a quarter pipe section (e.g., as in James et al. 2008) uniformly meshed with 0.05 m³ to 0.1 m³ cells (adjusted to keep computation times reasonable and small enough to resolve the falling film thickness). In each case, the volume-of-fluid method, with implicit body force enabled, was employed in a pressure-based solver, and thermal effects were also simulated. An explicit time-stepping method was used with the time-step fixed between 10⁻² and 10⁻³ s, and a

maximum Courant number of 0.25. A constant pressure upper boundary condition was used to represent the conduit at a depth of ≈ 100 m within the magma (2,750,025 Pa), and a zero-flow bottom boundary condition was imposed. Two fluids were simulated: magma (with temperature of 1000°C, e.g., Harris and Stevenson [1997], density of 2700 kg m³, e.g., Métrich et al., [2001] and surface tension of 0.4 N m²), and water vapour (for the slug, with thermal conductivity of 0.0261 W m⁻¹K⁻¹ and a ratio of specific heats of 1.4). Water vapour is the only compressible phase within the model and was chosen for the slug composition, as it is the dominant species in the volcanic gas chemistry (with 83% of the molar weight, Burton et al. [2007]).

Ansys Fluent® has previously been shown capable of modelling full 3D slug flow and daughter bubble production [e.g., Taha and Cui, 2006; Araujo et al. 2012], at engineering scales. To provide confidence in our quarter pipe model, a number of validation runs were performed (TC1 – TC5) to ensure that it replicated the five regimes of behaviour reported in Taha and Cui [2006] over N_f values of 84 – 1528. To reproduce the conditions of Taha and Cui [2006], these simulations used a pipe of radius 9.5 mm and length 190 mm, with liquids of surface tension 0.064 N m², densities ranging 1129 to 1223 kg m⁻³, and kinematic viscosities 9.7×10^{-5} to 5.47×10^{-6} m² s⁻¹. Dry air was used for the slug. Supplementary movie S2 demonstrates our model validation by showing matching wake features (i.e., an increasingly closed wake on decreasing N_f value and a commensurate decrease in turbulence in the wake area) and onset of daughter bubble production for each of the N_f values used by Taha and Cui [2006].

Following validation, 3D Stromboli-specific model runs (S1 – S12) were implemented for a range of magma viscosities (200, 300, 400, and 500 Pa s⁻¹), and conduit radii (1, 2, and 3 m), i.e., $N_f = 48 – 621$ [e.g., Vergnolle et al. (1996); Harris and Stevenson, (1997); Delle Donne and Ripepe, (2012)]. The initial slug and conduit lengths were set to ≈ 2.5 and 10 times the conduit radius, respectively (e.g., for $r_c = 2$ m, the conduit length was 20 m). These parameters were chosen to allow the flow regime to develop whilst minimising compute time and, by simulating slugs at depths ≈ 100 m, the effects of gas expansion did not substantially contribute to liquid motions. The magma density and viscosity values chosen here represent bulk column values; deviations from these values could occur through the presence of bubbles and crystals, with an increase in either of these acting to reduce N_f . The models were run in parallel on the University of Sheffield Linux high-performance computing cluster, with a total simulation time of < 2 weeks.

In five of these models, the production of daughter bubbles (see Table S2 for summary) was observed from the base of the rising slugs, to varying degrees (Fig. 3 and supplementary movie S3). These mass loss rates are stable for the duration of simulations, after a short initial start-up transient (Fig. 4) and ranged between $\approx 1.2 – 14.2$ kg s⁻¹ between the different models (Fig. 5a). For N_f values > 330 (models S5, S9, S10), slugs were observed to separate into four individual bubbles on initiation (see Fig. 3); this occurred for slugs that were wider than the maximum bubble diameter determined by theoretical considerations of bubble nose instability [Suckale et al., 2010] and is likely to be an artefact of the transient and unphysical conditions at model initiation (i.e. static fluid surrounding a stationary bubble). The possibility that daughter bubble production was triggered by similar transients in other models was tested by simulating a stable, non-daughter bubble producing slug (at $N_f \approx 100$, with $\mu = 1200$ Pa s and $r_c = 3$ m) for ≈ 10 s (i.e., so that a flow regime had fully developed), then decreasing the magma viscosity to 400 Pa s, to give $N_f = 310$. This resulted in a transition to daughter bubble production with rate similar to that generated if the model had originally been started with $N_f = 310$ (model S11).

Onset of daughter bubble production in our Stromboli models occurred at lower N_f values than in our validation models and in previous work [e.g. Noguiera et al., 2006; Taha and Cui, 2006]. The differences between the simulations are dominated by scale (from mm to m), surface tension (0.064 N m⁻² and 0.4 N m⁻²), and dynamic viscosity (two to three orders of magnitude difference). It is possible therefore that N_f does not fully capture all the physics required to parameterise daughter bubble production, and caution is required if extrapolating laboratory-scale results to volcanic scenarios.

4. Discussion

All the events measured at Stromboli had gas coda of $\approx 20 - 160$ s in duration, which in some cases contained post-explosive peaks in emission (e.g. Fig. 2c-f). As Stromboli persistently degasses, it is conceivable that the coda could result from interactions between the rising slug and gas already contained within the conduit [Gaudin et al. 2014]; for example, a pressure drop in the magma below a gas slug could allow additional gas exsolution in the wake region. If slugs are produced from regions of foam collapse or ascending pockets of gas saturated magma, bubble trains could also potentially be produced from ‘leftover’ bubbles following slug formation. Variability and flux peaks within coda could potentially be caused by the close rise and burst of independent bubbles or slugs, by gas dispersal processes in the upper conduit and atmosphere, or by complexities in slug burst due to heterogeneities in magma rheology [Del Bello et al., 2015; Capponi et al., 2016]. This said, given the efficiency of gas transfer from slugs into daughter bubbles demonstrated within our simulations, we do suggest that daughter bubble production could play a key role in driving coda generation in strombolian volcanism.

Our field measurements show that coda gas masses are $\approx 53 - 75$ % of total event gas masses (i.e., explosion plus coda) for Vent 1 events, and $\approx 70 - 84$ % for Vent 2 events (Fig. 1, using data between the 1st and 3rd quartiles of the distribution). Given the range of mass loss rates calculated from the simulations, $\approx 1.2 - 14.2$ kg s⁻¹, it is entirely plausible that coda on the order of those observed in our field measurements could be generated. We note that the gas mass loss rates for the Stromboli simulations do not show a straightforward relationship with N_f (Fig. 5a), further suggesting that work is warranted to characterise the processes behind slug mass loss rates. Future 3D models will also enable inclined conduit scenarios to be investigated, which would be of particular relevance to Stromboli, where the conduit is at 40° from the vertical [Chouet et al., 2003].

Daughter bubble production has interesting volcanological implications beyond the production of gas coda. Under conditions of sufficiently high N_f for daughter bubble production and shedding from the wake region, rising slugs will effectively dissipate during ascent. In this case, slugs may only substantially occur in the shallow portions of a conduit, where decompressive gas expansion can outweigh volumetric loss from daughter bubble production. At greater depths, ascending slug-sized gas pockets will dissipate until they transition to a stable morphology, such as cap bubbles, at which point the effective increase in falling film thickness and decrease in ascent velocity will reduce wake turbulence and hence mass loss [Wallis, 1969]. Furthermore, the release of daughter bubbles would add significant numbers of smaller bubbles to the conduit, some of which would coalesce (e.g., see models S7 and S12 in supplementary video 2) and, over greater flow distances than modelled here, could generate larger bubbles, providing an explanation for the post-explosive peaks in the flux data (Fig. 2). If slugs are sufficiently large, and a constant slug mass loss rate during ascent is assumed, then coda gas masses could be used to infer initial slug depths (Fig. 5b, c). If measured coda masses were generated from the smaller gas mass loss rates calculated in the simulations then (using slug rise speeds of $\approx 1.97 - 2.54$ m s⁻¹, see supplementary S1 for details) slugs could ascend from previously suggested formation depths of ~ 3 km [Burton et al. 2007; Chouet et al. 2008] while larger mass loss

rates would limit slug flow to depths < 1000 m (Fig. 5b). The Vent 2 coda masses are suggestive of much shallower source depths, as indicated in Fig. 5c, with the higher mass loss rates corresponding to depths < 100 m. This analysis, along with other characteristic gas mass differences between Vent 1 and Vent 2 events (Fig. 1h) suggests that the gas slugs driving each process may arise from different source regions or processes. However, the strong event variability, particularly for the Vent 1 explosions (Figs. 1g, and h), precludes more detailed interpretation from the current dataset and we encourage coda measurement to be integrated into longer term monitoring campaigns, with a view to substantially increasing the number of observations.

5. Conclusions

Using UV camera measurements of SO₂ gas fluxes from strombolian explosions, we demonstrate that a significant proportion of gas from each event can be contained within a flux coda that follows the initial explosively erupted gas mass. We suggest, supported by evidence from CFD simulations, that the observed flux coda could be generated by the production of daughter bubbles and the formation of a daughter bubble train that follows a rising slug. The production of daughter bubbles is demonstrated to vary with the inverse viscosity of the system, and potentially with conduit radius. Slugs of insufficient initial mass can dissipate into cap bubbles and a trailing bubble train prior to reaching the surface. This allows for the intriguing possibility that, in some systems, slug morphology can only be sustained in near-surface regions where depressurisation-driven gas expansion [James et al., 2008] exceeds gas volume loss to daughter bubbles.

Acknowledgements

T.D. Pering and A.J.S. McGonigle acknowledge the support of a NERC studentship (x/007002-14), the University of Sheffield and a Google Faculty Research award (r/136958-11-1). A. Aiuppa, D. Delle Donne, and G. Tamburello acknowledge support from the European Research Council starting independent research grant (agreement number 305377). Data used in the production of this work is available in the supplementary material and on the website of the corresponding author. We are finally grateful to Ed Llewellyn, Robin Campion and an anonymous reviewer for their reviews which have greatly improved the paper.

References

- Araújo, J.D.P., Miranda, J.M., Pinto, A.M.F.R., Campos, J.B.L.M., 2012. Wide-ranging survey on the laminar flow of individual Taylor bubbles rising through stagnant Newtonian liquids. *Int. J. Multiphase Flow* 43, 131–148.
- Blackburn, E.A., Wilson, L., Sparks, R.S.J., 1976. Mechanisms and dynamics of strombolian activity. *J. Geol. Soc.* 132, 429-440, DOI:10.1144/gsjgs.132.4.0429
- Bluth, G.J.S., Shannon, J.M., Watson, I.M., Prata, A.J., Realmuto, V.J., 2007. Development of an ultra-violet digital camera for volcanic SO₂ imaging. *J. Volcanol. Geotherm. Res.* 161, 47–56.
- Bouche, E., Vergnolle, S., Staudacher, T., Nercessian, A., Delmont, J.-C., Frogneux, M., 2010. The role of large bubbles detected from acoustic measurements on the dynamics of Erta 'Ale lava lake (Ethiopia). *Earth Planet. Sci. Letts* 295, 37-48, DOI:10.1016/j.epsl.2010.03.020
- Burton, M., Allard, P., Muré, F., La Spina, A., 2007. Magmatic gas composition reveals the source depth of slug-driven strombolian explosive activity. *Science* 317, 227–230.

- Campos, J.B., L.M., Guedes de Carvalho, J.R.F., 1988. An experimental study of the wake of gas slugs rising in liquids. *J. Fluid Mech.* 196, 27–37.
- Capponi, A., James, M.R., Lane, S.J., 2016. Gas slug ascent in a stratified magma: Implications of flow organisation and instability for Strombolian eruption dynamics. *Earth Planet. Sci. Letts* 435, 159-170, DOI:10.1016/j.epsl.2015.12.028
- Chouet, B., Hamisevicz, N., McGetchin, T. R., 1974. Photoballistics of volcanic jet activity at Stromboli, Italy. *J. Geophys. Res.* 279 (32), 4961-4976
- Chouet, B., Saccorotti, G., Dawson, P., Martini, M., Scarpa, R., De Luca, G., Milana, G., Cattaneo, M., 1999. Broadband measurements of the sources of explosions at Stromboli Volcano, Italy. *Geophys. Res. Lett.* 26 (13), 1937-1940.
- Chouet, B., Dawson, P., Ohminato, T., Martini, M., Saccorotti, G., Giudicepietro, F., De Luca, G., Milana, G., Scarpa, R., 2003. Source mechanisms of explosions at Stromboli Volcano, Italy, determined from moment-tensor inversions of very-long-period data, *J. Geophys. Res.* 108 (B1), DOI:10.1029/2002JB001919
- Chouet, B., Dawson, P., Martini, M., 2008. Shallow-conduit dynamics at Stromboli Volcano, Italy, imaged from waveform inversions. *Geol. Soc. Spec. Publ.*, 307, 57–84.
- Del Bello, E., Llewellyn, E.W., Taddeucci, J., Scarlato, P., Lane, S.J., 2012. An analytical model for gas overpressure in slug-drive explosions: insights into strombolian volcanic eruptions. *J. Geophys. Res.* 117 (B2), DOI:10.1029/2011JB008747.
- Del Bello, E., Lane, S.J., James, M.R., Llewellyn, E.W., Taddeucci, J., Scarlato, P., Capponi, A., 2015. Viscous plugging can enhance and modulate explosivity of strombolian eruptions. *Earth Planet. Sci. Letts* 423, 210-218, DOI:10.1016/j.epsl.2015.04.034
- Delle Donne, D, Ripepe, M., 2012. High-frame rate thermal imagery of Strombolian explosions: Implications for explosive and infrasonic source dynamics. *J. Geophys. Res.* 117 (B9), DOI:10.1029/2011JB008987
- Fernandes, R.C., Semiat, R., Dukler, A.E., 1983. Hydrodynamic model for gas-liquid slug flow in vertical tubes. *AIChE. J.* 29 (6), 981-989, DOI:10.1002/aic.690290617
- Gaudin, D., Taddeucci, J., Harris, A., Orr, T., Bombrun, M., Scarlato, P., 2014. When Puffing Meets Strombolian Explosions: A Tale of Precursors and Coda. In: EGU, Vienna General Assembly.
- Harris, A.J.L., Stevenson, D.S., 1997. Thermal observations of degassing open conduits and fumaroles at Stromboli and Vulcano using remotely sensed data. *J. Volcanol. Geotherm. Res.* 76, 175-198
- Horn B.K.P., Schunck B.G., 1981. Determining optical flow. *Artificial Intelligence*, 17, 185–203.
- James, M.R., Lane, S. J., Chouet, B., Gilbert, J.S., 2004. Pressure changes associated with the ascent and bursting of gas slugs in liquid-filled vertical and inclined conduits. *J. Volcanol. Geotherm. Res.* 129 (1-3), 61-82

- James, M.R., Lane, S.J., Chouet, B.A., 2006. Gas slug ascent through changes in conduit diameter: laboratory insights into a volcano-seismic source process in low-viscosity magmas. *J. Geophys. Res.* 111 (B05201), DOI:10.1029/2005JB003718.
- James, M.R., Lane, S.J., Corder, S.B., 2008. Modelling the rapid near-surface expansion of gas slugs in low-viscosity magmas. *Geol. Soc. Lond., Spec. Publ.* 307, 147–167.
- Kantzas, E.P., McGonigle, A.J.S., Tamburello, G., Aiuppa, A., Bryant, R.G., 2010. Protocols for UV camera volcanic SO₂ measurements. *J. Volcanol. Geotherm. Res.* 194, 55–60.
- Llewellyn, E.W., Del Bello, E., Taddeucci, J., Scarlato, P., Lane, S.J., 2012. The thickness of the falling film of liquid around a Taylor bubble. *Proc. R. Soc. B* 468. DOI:1098/rspa.2011.0476.
- Llewellyn, E.W., Burton, M., Mader, H., Polacci, M., 2014. Conduit speed limit promotes formation of explosive ‘super slugs’. In: San Francisco, AGU General Assembly.
- Métrich, N., Bertagnini, A., Landi, P., Rosi, M., 2001. Crystallization driven by decompression and water loss at Stromboli volcano (Aeolian Islands, Italy). *J. Petrol.* 42, 1471-1490.
- Mori, T., Burton, M., 2006. The SO₂ camera: a simple, fast and cheap method for ground based imaging of SO₂ in volcanic plumes. *Geophys. Res. Lett.* 33, L24804. DOI:10.1209/2006GL027916.
- Nogueira, S., Riethmuller, M.L., Campos, J.B.L.M., Pinto, A.M.F.R., 2006. Flow patterns in the wake of a Taylor bubble rising through vertical columns of stagnant and flowing Newtonian liquids: an experimental study. *Chem. Eng. Sci.* 61, 7199–7212.
- O'Brien, G. S., Bean, C.J., 2008. Seismicity on volcanoes generated by gas slug ascent. *Geophys. Res. Lett.* 35 (L16308), DOI:10.1029/2008GL035001
- Peters, N., Hoffmann, A., Barnie, T., Herzog, M., Oppenheimer, C., 2015. Use of motion estimation algorithms for improved flux measurements using SO₂ cameras. *J. Volcanol. Geotherm. Res.*, 300 300, 58-69, DOI:10.1016/j.volgeores.2014.08.031
- Ripepe, M., Harris, A. J. L., Carniel, R., 2002. Thermal, seismic and infrasonic evidences of variable degassing rates at Stromboli volcano. *J. Volcano. Geotherm. Res.* 118 (3-4), 285-297.
- Seyfried, R., Freundt, A., 2000. Experiments on conduit flow and eruption behaviour of basaltic volcanic eruptions. *J. Geophys. Res.* 105 (B10), 23,727–23,740.
- Suckale, J., Hager, B.H., Elkins-Tanton, L.T., Nave, J-C, 2010. It takes three to tango: 2. Bubble dynamics in basaltic volcanoes and ramifications for modelling normal Strombolian activity. *J. Geophys. Res.* 115 (B07410), DOI:10.1029/2009JB006917
- Taha, T., Cui, Z.F., 2006. CFD modelling of slug flow in vertical tubes. *Chemical Engineering Science* 61 (2), 676-687, DOI:10.1016/j.ces.2005.07.022
- Tamburello, G., Kantzas, E.P., McGonigle, A.J.S., Aiuppa, A., 2011. Recent advances in ground-based ultraviolet remote sensing of volcanic SO₂ fluxes. *Ann. Geophys.* 54 (2), 199–208.
- Tamburello, G., Aiuppa, A., Kantzas, E.P., McGonigle, A.J.S., Ripepe, M., 2012. Passive vs. active degassing modes at an open-vent volcano (Stromboli, Italy). *Earth Planet. Sci. Lett.* 359–360, 106–116.

Vergnolle, S., Brandeis, G., 1996. Strombolian explosions: 1. A large bubble breaking at the surface of a lava column as a source of sound. *J. Geophys. Res.* 101 (B9), 20,433–20,447.

Vergnolle, S., Brandeis, G., Mareschal, J.C., 1996. Strombolian explosions 2. Eruption dynamics determined from acoustic measurements. *J. Geophys. Res.* 101 (B9), 20,449–20,446

Viana, F., Pardo, R., Yáñez, R., Trallero, J.L., Joseph, D.D., 2003. Universal correlation for the rise velocity of long gas bubbles in round pipes. *J. Fluid Mech.* 494, 379–398.

Wallis, G.B., 1969. *One-dimensional Two-phase Flow*. McGraw-Hill, New York, NY.

Accepted Article

Figures, Tables and Captions

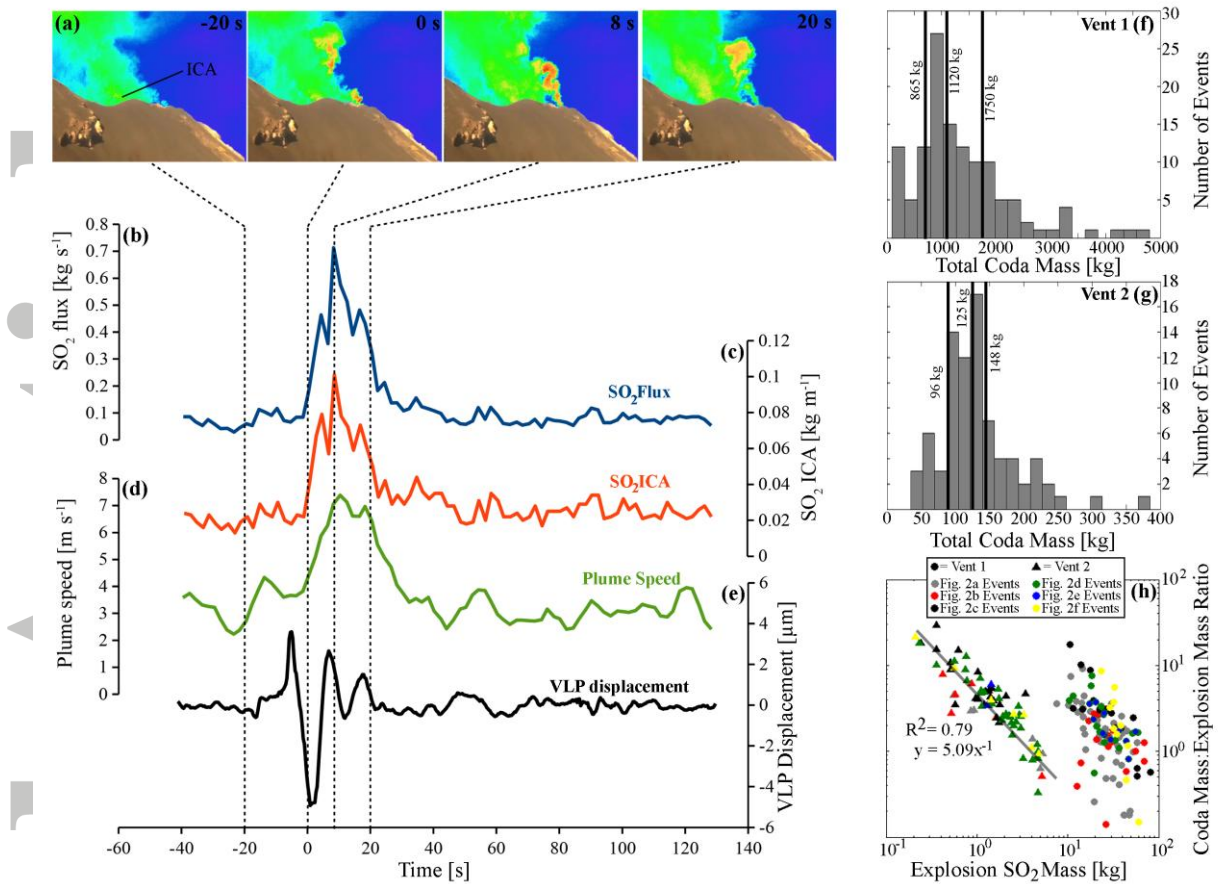


Figure 1: a) a sequence of UV camera images showing relative concentration of SO_2 , with line (at -20 s) showing where integrated column amount (ICA) is calculated; b) example SO_2 flux, c) ICA of SO_2 , d) plume speed, and e) VLP displacement for a single Vent 2 event. In f) and g) the distribution of coda masses for Vent 1 and Vent 2 events respectively, h) shows the relationship between SO_2 mass and coda:explosion mass ratio.

Accep

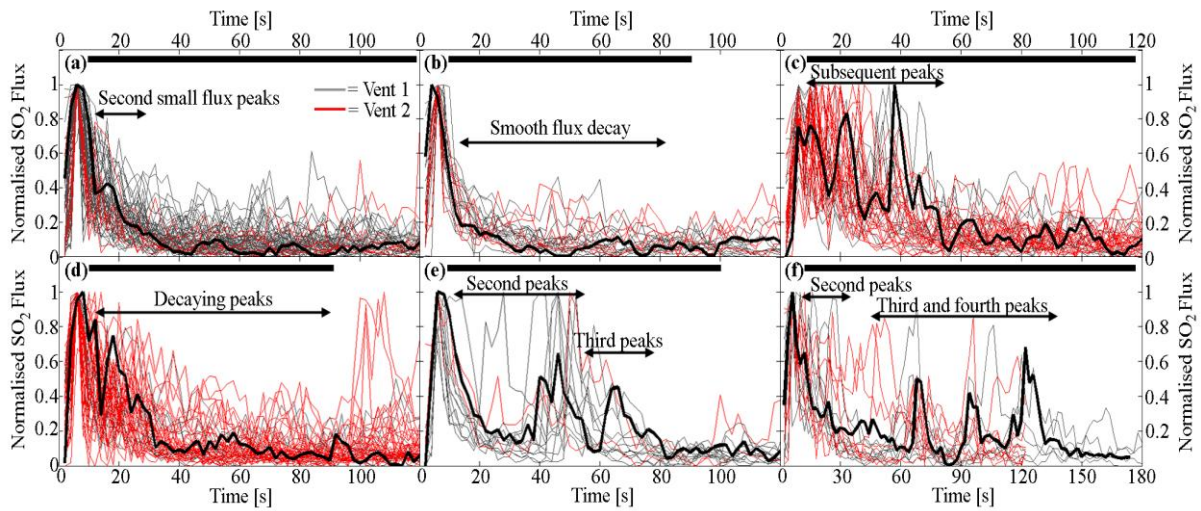


Figure 2: Graphs (a-e) summarising the characteristic degassing signatures observed following all Vent 1 and Vent 2 events. All events have been normalised by subtracting the minimum value and dividing by the maximum. The black horizontal bar at the top of the plots represents maximum event duration, while the thick black line traced on all subfigures represents a characteristic event. See supplementary Table S6 for details on how events were categorised.

Accepted

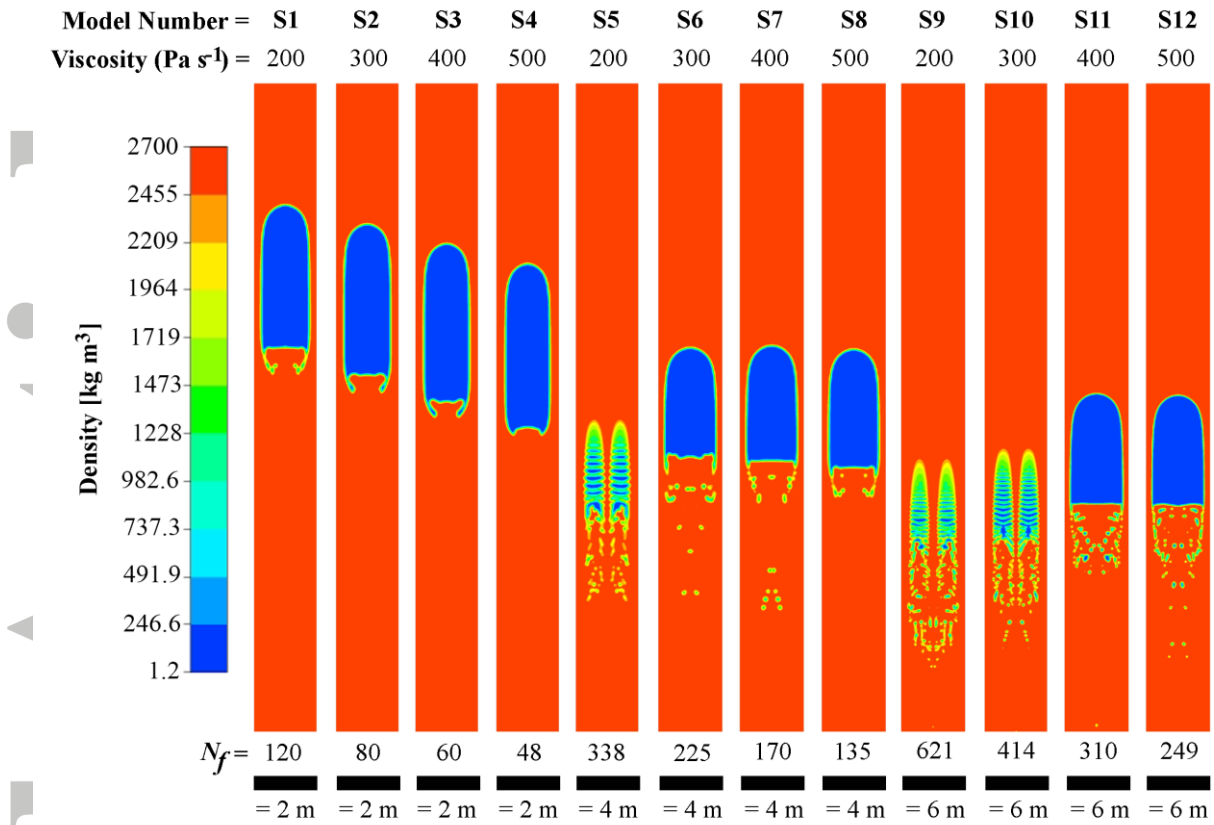


Figure 3: a) Example slug morphologies from the series of 3D simulations (S1 – S12). All models were captured at 10 s from initiation. Daughter bubble production is observed in several of the model runs.

Accepted

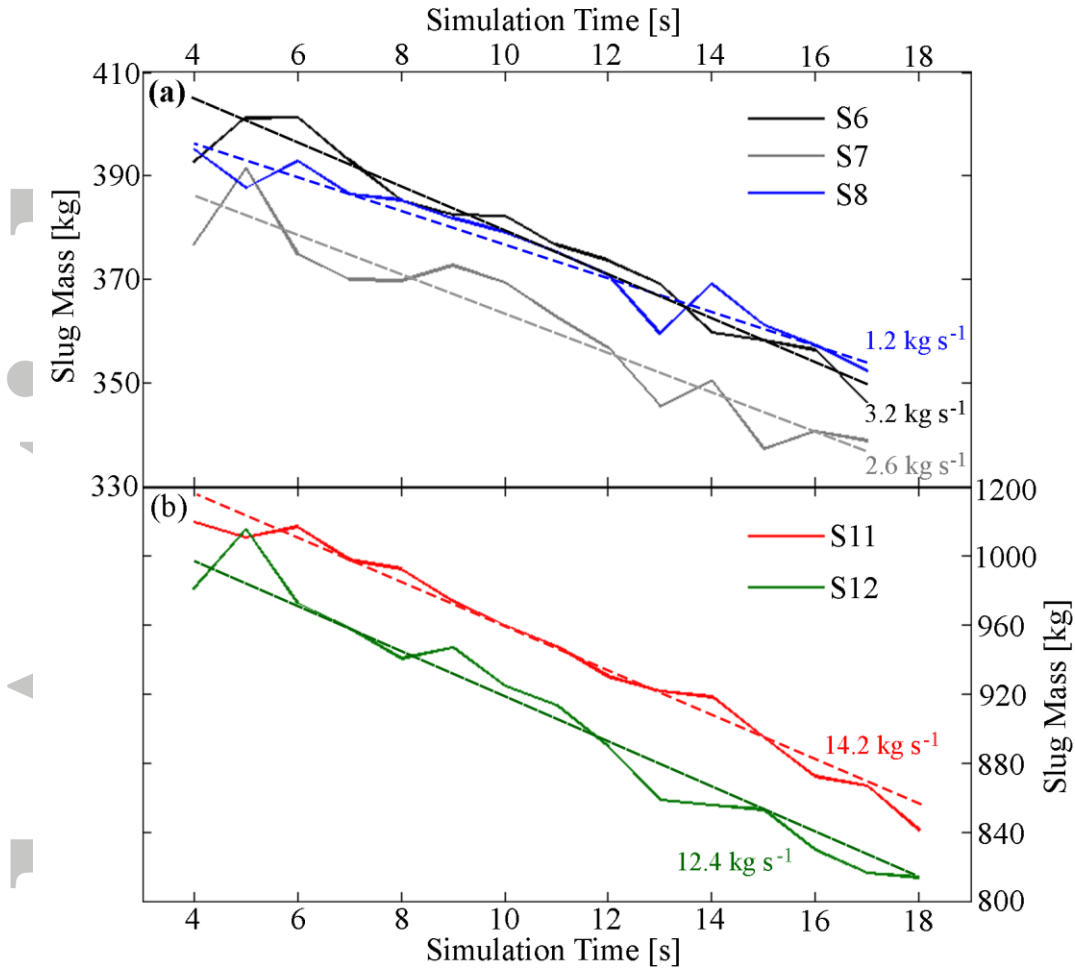


Figure 4: Slug gas mass during daughter bubble producing model runs. In a) model runs S6, S7, and S8 with $r_c = 2$ m. In b) S11, and S12 with $r_c = 3$ m. Dashed lines indicate linear best fit representing average mass loss rates (plotted against N_f in Fig. 5a).

Accep

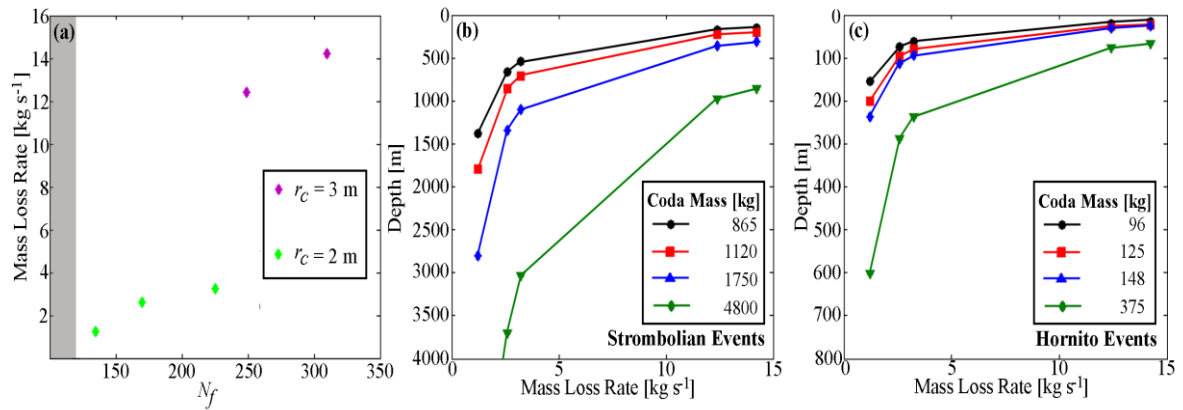


Figure 5: a) The relationship between gas mass lost from slugs per second and the dimensionless inverse viscosity, N_f , for daughter bubble producing model runs shaded region represents N_f values for simulations which did not produce daughter bubbles. In b) and c) the depths from which a slug must rise to generate coda masses representing the 1st quartile, median, 3rd quartile and maximum values of the measured distributions at Stromboli (Fig. 1f, g), for Vent 1 and Vent 2 events respectively.

Accepted